bioRxiv preprint doi: https://doi.org/10.1101/857953; this version posted November 29, 2019. The copyright holder for this preprint (which was not certified by peer review) is the author/funder. All rights reserved. No reuse allowed without permission.

Brain DNA Methylation Patterns in *CLDN5* Associated With Cognitive Decline

Anke Hüls, PhD[1], Chloe Robins, PhD[2], Karen N. Conneely, PhD[1], Rachel Edgar, BSc[3], Philip L. De Jager, MD, PhD[4,5], David A. Bennett, MD[6], Aliza P. Wingo, MD[7,8], Michael P. Epstein, PhD[1], Thomas S. Wingo, MD[1,2]

[1] Department of Human Genetics, Emory University, Atlanta, Georgia, USA

[2] Department of Neurology, Emory University School of Medicine, Atlanta, GA, US

[3] Centre for Molecular Medicine and Therapeutics, BC Children's Hospital Research Institute, and Department of Medical Genetics, University of British Columbia, Vancouver, British Columbia, Canada

[4] Cell Circuits Program, Broad Institute, Cambridge, MA, USA

[5] Center for Translational and Computational Neuroimmunology, Department of Neurology, Columbia University Medical Center, New York, NY, USA

[6] Rush Alzheimer's Disease Center, Rush University Medical Center, Chicago, Illinois, USA

[7] Division of Mental Health, Atlanta VA Medical Center, Decatur, GA, USA

[8] Department of Psychiatry, Emory University School of Medicine, Atlanta, GA, US

bioRxiv preprint doi: https://doi.org/10.1101/857953; this version posted November 29, 2019. The copyright holder for this preprint (which was not certified by peer review) is the author/funder. All rights reserved. No reuse allowed without permission.

Corresponding authors:

Aliza P. Wingo, M.D., M.Sc.
Atlanta VA Medical Center
1670 Clairmont Road, Decatur GA 30033
E-mail: Aliza.wingo@emory.edu

Michael P. Epstein, Ph.D.
305L Whitehead Building
615 Michael Street NE
Atlanta, GA 30322-1047
Email: mpepste@emory.edu

Thomas S. Wingo, M.D.
505K Whitehead Building
615 Michael Street NE
Atlanta, GA 30322-1047
Email: Thomas.wingo@emory.edu

Funding:

AH received a research fellowship from the Deutsche Forschungsgemeinschaft (DFG; HU 2731/1-1). MPE was supported by NIH grant R01 GM117946. APW is supported by NIH grants R01 AG056533, VA I01 BX003853, and NIH U01 MH115484. TSW was supported by NIH grants P50 AG025688, R56 AG062256, R56 AG060757, and R01 AG056533. CR was supported by NIH grant T32 NS007480. DAB was supported by P30AG10161, R01AG15819, R01AG17917, R01AG36042, U01AG61356. The funders had no role in the study design, data collection and analysis, decision to publish, or preparation of manuscript.

bioRxiv preprint doi: https://doi.org/10.1101/857953; this version posted November 29, 2019. The copyright holder for this preprint (which was not certified by peer review) is the author/funder. All rights reserved. No reuse allowed without permission.

Abstract

Objective: Cognitive decline is a hallmark of dementia; however, the brain epigenetic signature of cognitive decline is unclear. We investigated the associations between brain tissue-based DNA methylation and cognitive trajectory.

Methods: We performed a brain epigenome-wide association study of cognitive trajectory in 636 participants from the Religious Order Study and the Rush Memory and Aging Project (ROS/MAP) using DNA methylation profiles of the dorsal lateral prefrontal cortex (dPFC). To maximize our power to detect epigenetic associations, we used the recently developed Gene Association with Multiple Traits (GAMuT) test to analyze the five measured cognitive domains simultaneously.

Results: We found an epigenome-wide association for differential methylation of sites in the Claudin-5 (*CLDN5*) locus and cognitive trajectory (p-value = 9.96×10^{-7}), which was robust to adjustment for cell type proportions (p-value = 8.52×10^{-7}). This association was primarily driven by association with declines in episodic (p-value = 4.65×10^{-6}) and working memory (p-value = 2.54×10^{-7}). This association between methylation in *CLDN5* and cognitive decline was independent of beta-amyloid and neurofibrillary tangle pathology and present in participants with low levels of neuropathology. In addition, only 13-31% of the association between methylation and cognitive decline was mediated through levels of neuropathology, whereas the major part of the association was independent of it.

Interpretation: We identified methylation in *CLDN5* as new epigenetic factor associated with cognitive trajectory. Higher levels of methylation in *CLDN5* were associated with faster cognitive decline implicating the blood brain barrier in maintenance of cognitive trajectory.

bioRxiv preprint doi: https://doi.org/10.1101/857953; this version posted November 29, 2019. The copyright holder for this preprint (which was not certified by peer review) is the author/funder. All rights reserved. No reuse allowed without permission.

Introduction

Cognitive decline is a common concern among older adults; however, the trajectory of cognitive performance with age has a wide range from stable to rapid decline. Cognitive trajectory is an important predictor of health outcomes and mortality, independent of other commonly assessed risk factors[1]. Dementia is a common consequence of a decline in cognition, and Alzheimer Disease (AD) is its leading cause[2]. AD is characterized by the neuropathological accumulation of neuritic plaques and neurofibrillary tangles, which is accompanied by neuronal loss[3]; however, most older individuals have several co-occurring neuropathologies. Collectively, neuropathologies explain about 40% of the variance in cognitive trajectory, leaving most unexplained[4,5]. Thus, cognitive trajectory may be considered a summation of the different neuropathological and biological processes independent of pathologies at work in the aging human brain[5–7].

Despite the importance of understanding cognitive trajectory, existing epigenetic work on DNA methylation levels measured in brain tissue has primarily focused on AD-specific pathologies [8–11] and clinical diagnosis of AD [12–14]. In contrast, epigenetic studies that focused on examining cognitive decline were limited due to measuring DNA methylation changes in blood[15], which showed only moderate correlations (~0.4) with brain methylation[15]. Thus, there is need to understand the epigenetic changes that are associated with cognitive trajectory to identify potential mechanisms that may act through or independent of known neuropathologies.

In this study, we investigated the associations between brain tissue-based DNA methylation and cognitive trajectory in 636 participants from the Religious Order Study and Rush Memory and Aging Project (ROS/MAP) cohorts. Cognitive trajectory was assessed in five cognitive domains (episodic memory, perceptual speed, perceptual orientation, semantic memory, and working memory), which were analyzed simultaneously by using an innovative

bioRxiv preprint doi: https://doi.org/10.1101/857953; this version posted November 29, 2019. The copyright holder for this preprint (which was not certified by peer review) is the author/funder. All rights reserved. No reuse allowed without permission.

kernel procedure that allows to investigate associations between multiple predictors (e.g. methylation sites in a gene) with multiple outcomes (e.g. multiple cognitive domains) [16,17]. Findings were validated in independent post-mortem frontal cortex samples[10], and their biological plausibility were evaluated using gene expression and genotype data.

Methods

Study design and study population

The discovery dataset included deceased subjects from two large, prospectively followed cohorts recruited by investigators at Rush Alzheimer's Disease Center in Chicago, IL: The Religious Orders Study (ROS) and the Rush Memory and Aging Project (MAP)[11,18]. Both ROS and MAP collect detailed annual cognitive and clinical evaluations, and brain autopsy. Participants provided informed consent, an Anatomic Gift Act for organ donation, and a repository consent to allow their data to be repurposed. Both studies were approved by an Institutional Review Board of Rush University Medical Center. To be included in the present study, participants must have at least two follow-up evaluations, and available methylation data derived from dorsolateral prefrontal cortex. As in previous publications, the ROS and MAP data were analyzed jointly since much of the phenotypic data collected are identical at the item level in both studies and collected by the same investigative team[11,19].

The replication dataset included samples from the MRC London Neurodegenerative Disease Brain Bank (GSE59685)[10].

DNA methylation

In the discovery dataset, DNA methylation was measured from the dorsolateral prefrontal cortex (dPFC; Broadman area 46) as previously described in 737 ROS/MAP

bioRxiv preprint doi: https://doi.org/10.1101/857953; this version posted November 29, 2019. The copyright holder for this preprint (which was not certified by peer review) is the author/funder. All rights reserved. No reuse allowed without permission.

121 participant samples [11], of which 665 had complete phenotype and covariate information. DNA
122 was extracted from cortically dissected sections of dPFC and DNA methylation was measured
123 using the Illumina HumanMethylation450 Beadchip array. Initial data processing, including
124 color channel normalization and background removal, was performed using the Illumina
125 GenomeStudio software. The raw IDAT files were obtained from Synapse
126 (www.synapse.org; Synapse ID: syn7357283) and the following probes were removed: 1)
127 probes with a detection p-value > 0.01 in any sample, 2) probes annotated to the X and Y
128 chromosomes by Illumina, 3) probes that cross-hybridize with other probes due to sequence
129 similarity (identified by [20]), 3) non-CpG site probes, and 4) probes that overlap with common
130 SNPs (identified by [21]). After this filtering, the remaining CpG sites were normalized using
131 the BMIQ algorithm in Watermelon R package[22], and the ComBat function from the sva R
132 package was used to adjust for batch effects[23]. CpG sites with a distance of more than 20 KB
133 to the closest gene were excluded from analysis. After quality control 338,036 discrete CpG
134 dinucleotides corresponding to 26,558 genes in 636 subjects were used for analysis.

135 In the replication dataset, DNA methylation was derived from prefrontal cortex
136 obtained from individuals archived in the Medical Research Counsil (MRC) London
137 Neurodegenerative Disease Brain Bank. This previously published dataset provided samples
138 with DNA methylation data measured on the Illumina HumanMethylation450 Beadchip array.
139 Data was obtained from the Gene Expression Omnibus (GEO; GSE59685)[10]. Similar to above
140 probes annotated to the X and Y chromosomes, cross-hybridizing probes, non-CpG site
141 probes and probes that overlap with common SNP were removed. The data downloaded from
142 GEO was already normalized using the dasen algorithm in Watermelon R package[22] and then
143 the ComBat function from the sva R package was used to adjust for array ID batch effects [23].
144 Neuronal and non-neuronal brain cell-type proportions were estimated and normalized
145 between PFC samples[24]. CpG sites with a distance of more than 20 KB to the closest gene

bioRxiv preprint doi: https://doi.org/10.1101/857953; this version posted November 29, 2019. The copyright holder for this preprint (which was not certified by peer review) is the author/funder. All rights reserved. No reuse allowed without permission.

were excluded from analysis. After quality control 358,515 discrete CpG dinucleotides corresponding to 27,585 genes in 66 subjects were used for analysis.

Genotype data

Genotyping data was generated using two microarrays, Affymetrix GeneChip 6.0 (Affymetrix, Inc, Santa Clara, CA, USA) and Illumina HumanOmniExpress (Illumina, Inc, San Diego, CA, USA) as described previously[25]. Genotyping was imputed to the 1000 Genome Project Phase 3 using the Michigan Imputation Server [26], and the following filtering criteria were applied minor allele frequency (MAF) > 5%, Hardy-Weinberg p-value $>10^{-5}$ and genotype imputation $R^2 > 0.3$.

Gene expression

RNA extracted from ROS/MAP post-mortem dPFC was sequenced on the Illumina HiSeq with 101-bp paired-end reads using the strand-specific dUTP method with poly-A selection with a coverage of 50 million reads. BAM files were converted to FASTQ format using Picard, followed by alignment of reads to GRCh38 reference genome using STAR[27]. Gene level counts were computed using STAR[27]. Genes with < 1 count per million in at least 50% of the samples and with missing length and percent GC content were removed. Additionally, two outlier samples were removed. After quality control, counts were normalized using variance stabilization transformation, which performed $\log_2$ transformation of the counts, normalizes for library size, and transforms the counts to approximately homoscedastic [28]. Then the candidate mRNAs were extracted for association analysis with rate of cognitive decline adjusting for sex, age at death, RIN, PMI, RNA-sequencing batch, and cell type composition. Proportions of neurons, astrocytes, oligodendrocytes, and

bioRxiv preprint doi: https://doi.org/10.1101/857953; this version posted November 29, 2019. The copyright holder for this preprint (which was not certified by peer review) is the author/funder. All rights reserved. No reuse allowed without permission.

170 microglia were estimated from RNA-sequencing data using CIBERSORT[29] and cell-type
171 specific signatures[30]. We used the proportions of cell type to adjust for tissue heterogeneity.
172 Using the findings of the epigenome-wide association study of cognitive trajectory, we
173 selected the transcripts corresponding to the associated genes for further analyses after the
174 aforementioned quality control and variance stabilization transformation.

175

176 *Cognitive trajectory*

177 Cognitive trajectory was assessed in five different cognitive domains: episodic
178 memory, perceptual speed, perceptual orientation, semantic memory, and working memory.
179 Participants in both studies underwent structured, annual clinical evaluations that included
180 detailed cognitive and neurologic examinations, as previously reported [31,32]. Scores from
181 those tests were converted to z-scores using the mean and standard deviation of the cohorts at
182 baseline. Cognitive scores were modeled longitudinally with a mixed effects model, adjusting
183 for age, sex and education, providing person-specific random slopes of decline. The random
184 slope of each subject captures the individual rate of cognitive decline after adjusting for age,
185 sex and education.

186

187 *Neuropathologic Outcomes*

188 We used the CERAD score and Braak staging as neuropathological outcomes in our
189 analyses. The CERAD score is a semiquantitative measure of neuritic plaque density as
190 recommended by the Consortium to Establish a Registry for Alzheimer's Disease (CERAD).
191 A CERAD neuropathological diagnosis of AD requires moderate (probable AD) or frequent
192 neuritic plaques (definite AD) in one or more neocortical regions. The Braak stage is a
193 standardized measure of neurofibrillary tangle distribution and burden determined at autopsy

bioRxiv preprint doi: https://doi.org/10.1101/857953; this version posted November 29, 2019. The copyright holder for this preprint (which was not certified by peer review) is the author/funder. All rights reserved. No reuse allowed without permission.

194 with modified Bielschowsky silver stained sections[33]. Braak stages I and II indicate
195 neurofibrillary tangle confined mainly to the entorhinal region of the brain, Braak stages III
196 and IV indicate involvement of limbic regions such as the hippocampus and Braak stages V
197 and VI indicate moderate to severe neocortical involvement.

198

199 *Statistical analysis*

200 In our main analysis, we estimated epigenetic associations across five neurocognitive
201 domains in a gene-based analysis, in which each CpG site was assigned to the closest gene
202 using the Bioconductor package hiAnnotator[34] and the ensembl gene predictions (ensGene,
203 version of Apr-06-2014). All CpG sites with a distance of no more than 20 KB to the closest
204 gene, were included in the analyses. In addition, we conducted a sensitivity analysis in which
205 we only included CpG sites with a distance of no more than 10 KB to the closest gene. In a
206 traditional association study of cognitive trajectory, each cognitive test may be either tested
207 individually [15] or used to estimate a composite measure aggregated across several cognitive
208 tests[35]. However, these approaches are underpowered in the presence of pleiotropy since they
209 fail to exploit correlation among domains[17]. Thus, analysis of a single composite measure can
210 lose power if the causal CpG sites are only associated with a subset of the features that make
211 the composite measure[17]. Hence, it can be more powerful to directly account for the trait
212 correlations using kernel methods[36]. Kernel methods quantify the genetic similarity among
213 pairs of subjects and test whether this genetic similarity is associated with trait similarity.
214 Thus, they harness potential pleiotropy that exists between traits to improve power to detect
215 associations. To analyze epigenetic associations across five neurocognitive domains
216 simultaneously, we applied a variation of the GAMuT test [16] that was adapted to DNA
217 methylation data. GAMuT is motivated by the idea that individuals with similar epigenetic
218 patterns should also have similar cognitive traits across the different cognitive domains.

bioRxiv preprint doi: https://doi.org/10.1101/857953; this version posted November 29, 2019. The copyright holder for this preprint (which was not certified by peer review) is the author/funder. All rights reserved. No reuse allowed without permission.

Consequently, GAMuT constructs two different similarity matrices; one similarity matrix including cognitive decline in the five cognitive domains and the other similarity matrix for the epigenetic variation (beta values of CpG sites) assigned to a gene. Phenotypic and epigenetic similarity were modelled using linear kernels. P-values for GAMuT were derived using Davies' exact method, which is a computationally efficient method to provide accurate p-values in the extreme tails of tests that follow mixtures of chi-square variables [37,38]. To test which cognitive domains and CpG sites were likely main drivers in our multivariate analysis, we conducted an association analysis for each domain separately. The gene-based analyses for the single domains were performed with GAMuT and linear regression analyses were used in the CpG-based analyses.

All association models were adjusted for age at death, education, sex, ancestry, smoking status and post-mortem interval (PMI). Principal components (PCs) based on CpG sites chosen for their potential to proxy nearby SNPs (within 10 BP) were used to correct for population stratification (first three PCs, Figure S1) and cell type heterogeneity [21]. Samples whose first PC (PC1) deviated more than 3 standard deviations from the mean PC1, were excluded from analyses, reducing the final sample size from 665 to 636. In a sensitivity analysis, associations were additionally adjusted for cell type proportions[24]. All analyses were performed using R (version 3.4.3) using built-in functions unless otherwise specified.

We applied a Bonferroni threshold to correct for multiple testing. In the gene-based GAMuT analysis, the significance threshold was adjusted for the number of tested genes (threshold: $0.05/26{,}558 = 1.88 \times 10^{-6}$) and in the CpG-site-based linear regression analyses for the number of tested CpG sites (threshold: $0.05/338{,}036 = 1.48 \times 10^{-7}$).

Methylation signals associated with cognitive decline were validated using CERAD and Braak stage as outcomes. In addition, we analyzed whether the association between methylation and cognitive decline was modified (interaction analysis) or mediated (causal

bioRxiv preprint doi: https://doi.org/10.1101/857953; this version posted November 29, 2019. The copyright holder for this preprint (which was not certified by peer review) is the author/funder. All rights reserved. No reuse allowed without permission.

mediation analysis) by neuropathology (CERAD, Braak stage). Causal mediation analysis from a counterfactual perspective was performed by using the R package "mediation" [39], an approach that relies on the quasi-Bayesian Monte Carlo method based on normal approximation [40]. Using the counterfactual framework allows for definition of direct and indirect effects and a total effect as the sum of direct and indirect effects. The indirect effect refers to the effect through the mediator under study. The direct effect refers to the remaining effect that is not through the mediator [41]. The proportion of the indirect effect in the total effect was used to assess the extent to which the association between methylation and cognitive decline was mediated through neuropathology as an intermediate pathway [42].

The replication dataset did only have Braak stage as neurocognitive outcome, which is strongly associated with cognitive decline [33]. In the replication dataset, associations between CpG sites within a gene and the Braak stage were tested with GAMuT after correction for age at death, sex and cell type composition. Due to the small sample size of the replication dataset, we conducted a permutation test with 10,000 replications in addition to the Davies' approximation to verify the accuracy of p-values.

The biological plausibility of our findings was examined by investigating the association 1) of DNA methylation with gene expression as well as of gene expression with cognitive decline and 2) of genotypes with cognitive decline to investigate if our associations were due to a hidden genotype effect. All of these associations were tested using GAMuT and the genotype associations were followed by a linear regression analysis on the single SNP level. Fine-mapping of our epigenome-wide associations was done with coMET [43], which is a visualization tool of EWAS results with functional genomic annotations and estimation of co-methylation patterns.

Results

bioRxiv preprint doi: https://doi.org/10.1101/857953; this version posted November 29, 2019. The copyright holder for this preprint (which was not certified by peer review) is the author/funder. All rights reserved. No reuse allowed without permission.

Description of study participants

There were 636 ROS/MAP participants included in this study with an average age at death of 86 years and with 63% being female (Table 1). Most of the participants were white (98%), had a high level of education and 70% had never smoked. On average, cognitive performance declined with age for every single domain (Table 1) and correlations of cognitive decline between different domains were moderate, ranging from 0.54 to 0.78 (Table S1). Cognitive decline was associated with more signs of neuropathology (CERAD and Braak stage, Table S2).

There were 66 MRC Brain Bank participants with an average age at death of 87 years, with 67% being female and an average Braak stage of 5 (Table 1).

Methylation patterns of CLDN5 associated with cognitive decline

In the ROS/MAP participants (discovery dataset), we found that methylated CpG sites in the Claudin-5 (*CLDN5*) locus were associated with cognitive trajectory (p-value = 9.96×10^{-7}; Figure 1, Table 2, Table S3, and Figure S1). This association was robust to adjustment for cell type proportions (p-value = 8.52×10^{-7}, Table S4, Figures S2 and S3), to the selection of a smaller window of CpG sites around each gene (p-value = 9.96×10^{-7}, within 10kb, Table S5), and to the restriction to participants with European ancestry (621/636 participants, p-value = 9.73×10^{-7}, Table S6). The trajectories of episodic and working memory were the main drivers for the observed association with both being associated with CpG sites assigned to *CLDN5* in the analyses of the single domains (Table 2, Figure S4 and Tables S7-S11). Genes showing suggestive association with cognitive trajectory (p-values < 5×10^{-5}) included *AC084018.1, CTB-186G2.1, ATG16L2, KCNN4, RP11-779O18.1, TTC22, DCUN1D2-AS, PNMA1 and RP11-101C11.1*. The strongest associations with these genes were found with

bioRxiv preprint doi: https://doi.org/10.1101/857953; this version posted November 29, 2019. The copyright holder for this preprint (which was not certified by peer review) is the author/funder. All rights reserved. No reuse allowed without permission.

episodic memory, followed by working memory. Interestingly, most top methylation signals in Table 2 (*CLDN5* and 7/9 suggestive genes) were also at least nominally associated with CERAD (Table 3, Figures S5-S6 and Table S12) and Braak stage (Table 3, Figure S7 and Table S13).

To generalize our findings from the ROS/MAP participants, we performed the same epigenetic analysis in MRC Brain Bank participants with DNA methylation data available (replication dataset). We tested for differential methylation using Braak stage. Of the 8 methylation signals, which were at least nominally associated with Braak stage in the discovery dataset, *CLDN5*, *CTB-186G2.1* and *KCNN4* could be replicated in the replication dataset (Table 3, Table S14, Figure S8).

Higher levels of methylation in CLDN5 locus associated with cognitive decline

To identify which CpG sites are the main drivers of the observed associations and to understand the direction of association, we conducted a linear regression analysis for the cognitive trajectory of each cognitive domain. Interestingly, except for *PNMA1*, higher levels of methylation within our top genes were associated with an increased cognitive decline in every single cognitive domain (Table S15). Within the CpG sites assigned to *CLDN5*, cg16773741 and cg05460329 were the main drivers of the association with cg16773741 being associated with episodic memory (p-value = 1.48×10^{-8}), semantic memory (8.81×10^{-8}) and working memory (8.66×10^{-9}) (Table 4). The direction of association with these two CpG sites was consistent with the association observed for CERAD and Braak stage, which could further be replicated in the replication dataset (Table S15, N=66).

Association with CLDN5 even present without signs of neuropathology

bioRxiv preprint doi: https://doi.org/10.1101/857953; this version posted November 29, 2019. The copyright holder for this preprint (which was not certified by peer review) is the author/funder. All rights reserved. No reuse allowed without permission.

To investigate if the association between methylation in CLDN5 and cognitive decline is also present in participants without clear signs of neuropathology, we conducted an analysis of the interaction between the most significantly associated CpG site (cg16773741) and CERAD or Braak stage on cognitive decline. The association between methylation in cg16773741 did not significantly differ between participants with no to little signs of neuropathology versus participants with moderate to severe signs of neuropathology (measured by CERAD and Braak stage; Figure 3). Consequently, the association between methylation in cg16773741 and decline in episodic, semantic, and working memory was even significant in participants with no or little signs of neuropathology..

Partial mediation through neuropathology

The association between DNA methylation in the *CLDN5* locus (cg16773741) and cognitive trajectory was only partially mediated through an increased neuropathology. It ranged between 17% (95% confidence interval (CI): 18-40%) to 31% (95% CI: 18-61%) for CERAD and 13% (95% CI: 7-21%) to 27% (95% CI: 15-41%) for Braak stage depending on the cognitive domain (Figure 4). Therefore, the major part of the association with *CLDN5* was a direct association between methylation and cognitive decline, which was independent of beta-amyloid and neurofibrillary neuropathology.

Methylation signals were independent of genotypes

Genotypes located within the windows of *CLDN5* were associated with DNA methylation (p-value < 10^{-6}), but not with cognitive trajectory (p-value = 0.4415, Table S16 A). In line, associations of DNA methylation in the *CLDN5* window with cognitive trajectory were robust to adjustment for genotypes from the same window (Table S16 B).

bioRxiv preprint doi: https://doi.org/10.1101/857953; this version posted November 29, 2019. The copyright holder for this preprint (which was not certified by peer review) is the author/funder. All rights reserved. No reuse allowed without permission.

This observation was confirmed by the subsequent analyses on the single CpG / SNP level, which showed that the CpG sites associated with genotypes were not the same as being associated with cognitive trajectory (Table S17, Figure 2 and Figures S9 to S12). This indicates that our methylation signals were not caused by hidden genotype effects.

No clear association with gene expression levels

In our sample, we find no association between DNA methylation in the *CLDN5* window and *CLDN5* expression (p-value = 0.1978; Table S17). *KCNN4* was the only top gene (Table 2) for which methylation levels were associated with expression levels (p-value = 0.0004; Table S18). Furthermore, cognitive trajectory was not associated with expression of any gene in Table 2 (Table S18).

Discussion

In this study, we found an epigenome-wide association between brain-tissue-based DNA methylation in the *CLDN5* locus and cognitive trajectory in more than 600 participants from the ROS/MAP cohort. This association was significant across different domains and particularly associated with trajectories in episodic and working memory. We also found that higher levels of methylation in *CLDN5* were associated with neuropathology in our discovery and replication datasets consistent with the direction of association found with cognitive decline. Most interestingly, the association between methylation in CLDN5 and cognitive decline was independent of beta-amyloid and neurofibrillary neuropathology and even present in participants with low levels of those pathologies. In addition, only 13-31% of the association between methylation and cognitive decline was mediated through levels of neuropathology, whereas the major part of the association was independent of it. Finally, we

bioRxiv preprint doi: https://doi.org/10.1101/857953; this version posted November 29, 2019. The copyright holder for this preprint (which was not certified by peer review) is the author/funder. All rights reserved. No reuse allowed without permission.

365 found no evidence that hidden effects of genotypes in the *CLDN5* locus confounded our
366 methylation results.

367 *CLDN5* is an integral membrane protein and an important component of tight junction
368 protein complexes that comprise the blood-brain barrier. The blood-brain barrier is located at
369 endothelial cells lining the brain microvasculature and is maintained by the neurovascular
370 unit, a functional relationship between astrocytes, neurons, and endothelial cells [44].
371 Dysfunction of the blood-brain barrier has been implicated in neurodegenerative disorders,
372 such as AD [44–47]. Thus, our finding that altered regulation of *CLDN5* is associated with
373 cognitive decline suggests a role of blood-brain barrier dysfunction in cognitive decline. We
374 note that an estimated two-thirds of AD dementia (clinically defined) and that an estimated
375 40% of cognitive decline are attributable to known age-related neuropathologies [4,48]. Thus,
376 our findings may account for some of the unaccounted-for variation in cognitive decline and
377 AD dementia.

378 This is the first epigenome-wide study using cognitive trajectory in older individuals.
379 A previous study on the same cohort showed an association of 71 CpG sites with neuritic
380 plaque burden, of which 11 were validated in an independent cohort[11]. Here, we showed that
381 all of these 11 signals were at least nominally associated with cognitive trajectory and the
382 strongest associations were again found for cognitive trajectory of episodic and working
383 memory (Table S19). In addition, we identified methylation in *CLDN5* as new epigenetic
384 factor associated with cognitive trajectory, a gene that has not been linked to AD in a
385 population-based cohort.

386 By contrast, associations of blood-based methylation levels with global cognitive
387 function (cg21450381) and phonemic verbal fluency (cg12507869) [15] could not be validated
388 in our study (Table S20). The likely reasons are the different source of methylation data, and

bioRxiv preprint doi: https://doi.org/10.1101/857953; this version posted November 29, 2019. The copyright holder for this preprint (which was not certified by peer review) is the author/funder. All rights reserved. No reuse allowed without permission.

differences in the phenotype (i.e., cognitive trajectory over time in our study versus cognitive testing at a single time point[15]).

Strengths of this study include the ROS/MAP cohort as a discovery dataset which is notable for its longitudinal nature with very high follow-up rates, prospective collection of data, a community-based cohort design, and detailed neuropathological examination following high autopsy rates. The validity of our signals was also determined in an independent replication dataset, and the availability of genomic data allowed us to determine methylation changes were not the result of hidden genotype effect. This study is also strengthened by the GAMuT [16] statistical method that harnesses correlations among cognitive domains and among CpG sites to improve statistical power compared to standard univariate techniques.

The study is potentially limited by its cross-sectional nature. Although brain tissue is the ideal target tissue to measure DNA methylation related to cognitive trajectory, it inhibited a simultaneous (or even later) assessment of cognitive function. Consequently, we cannot exclude the potential risk of reverse causality in our associations. Another potential limitation is the use of bulk tissue analysis which might obscure signals from different cell populations. This problem was mitigated in our analysis by adjusting for cell-type composition. However, the bulk tissue analysis may have obscured an association between *CLDN5* methylation and RNA expression. Future studies should investigate the role of *CLDN5* in specific cell types from brain and investigate whether there is a causal relationship between *CLDN5* dysregulation and cognitive decline in animal models of AD.

In conclusion, we have presented evidence for brain-based DNA methylation in association with cognitive trajectory. We identified methylation in *CLDN5* as a new epigenetic factor associated with cognitive trajectory, which was validated in an independent dataset and independent of beta-amyloid and neurofibrillary neuropathology. Higher levels of

bioRxiv preprint doi: https://doi.org/10.1101/857953; this version posted November 29, 2019. The copyright holder for this preprint (which was not certified by peer review) is the author/funder. All rights reserved. No reuse allowed without permission.

414 methylation in *CLDN5* were associated with cognitive decline implicating the blood brain
415 barrier in maintenance of cognitive trajectory with aging.

bioRxiv preprint doi: https://doi.org/10.1101/857953; this version posted November 29, 2019. The copyright holder for this preprint (which was not certified by peer review) is the author/funder. All rights reserved. No reuse allowed without permission.

Acknowledgments:

The authors are grateful to the participants of the Rush Memory and Aging Project and Religious Orders Study and the Medical Research Counsel Brain Bank.

Author Contributions:

AH planned and conducted the analyses supported by MPE, KC, TSW and APW. AH, TSW, APW and MPE were the major contributors in writing the manuscript. KC and CR were responsible for the preprocessing and quality control of the DNA methylation data from the discovery cohort and RE for the replication cohort. APW conducted the preprocessing and quality control of the RNAseq data and TSW was supervised the quality control of the genotype data. PLDJ generated the methylation, transcriptomic, and genetic data. DAB conceived, designed, and leads the ROS/MAP study and the methylation sub-study.

Competing financial interests declaration:

The authors have nothing to declare.

Web resources:

Data used in this study: https://www.synapse.org/#!Synapse:syn2580853

Rush Alzheimer's Disease Center Research Resource Sharing Hub: www.radc.rush.edu.

Epstein Software: https://github.com/epstein-software.

MRC London Neurodegenerative Diseases Brain Bank:

https://www.kcl.ac.uk/ioppn/depts/bcn/our-research/neurodegeneration/brain-bank.

Ensembl gene predictions (ensGene, version of Apr-06-2014):

http://hgdownload.soe.ucsc.edu/goldenPath/hg19/database/.

bioRxiv preprint doi: https://doi.org/10.1101/857953; this version posted November 29, 2019. The copyright holder for this preprint (which was not certified by peer review) is the author/funder. All rights reserved. No reuse allowed without permission.

References

1. Batty GD, Deary IJ, Zaninotto P. Association of cognitive function with cause-specific mortality in middle and older age: Follow-up of participants in the english longitudinal study of ageing. Am. J. Epidemiol. 2016;183(3):183–190.
2. Van Cauwenberghe C, Van Broeckhoven C, Sleegers K. The genetic landscape of Alzheimer disease: Clinical implications and perspectives. Genet. Med. 2016;18(5):421–430.
3. Möller HJ, Graeber MB. The case described by Alois Alzheimer in 1911. Historical and conceptual perspectives based on the clinical record and neurohistological sections. Eur. Arch. Psychiatry Clin. Neurosci. 1998;248(3):111–22.
4. Boyle PA, Wilson RS, Yu L, et al. Much of late life cognitive decline is not due to common neurodegenerative pathologies. Ann. Neurol. 2013;74(3):478–489.
5. Boyle PA, Yu L, Wilson RS, et al. Person-specific contribution of neuropathologies to cognitive loss in old age. Ann. Neurol. 2018;83(1):74–83.
6. Schneider JA, Aggarwal NT, Barnes L, et al. The neuropathology of older persons with and without dementia from community versus clinic cohorts. J. Alzheimer's Dis. 2009;18(3):691–701.
7. Terry RD, Masliah E, Salmon DP, et al. Physical basis of cognitive alterations in Alzheimer's disease: synapse loss is the major correlate of cognitive impairment. Ann. Neurol. 1991;30(4):572–80.
8. Li P, Marshall L, Oh G, et al. Epigenetic dysregulation of enhancers in neurons is associated with Alzheimer's disease pathology and cognitive symptoms. Nat. Commun. 2019;10(1):1–14.
9. Altuna M, Urdánoz-Casado A, Sánchez-Ruiz De Gordoa J, et al. DNA methylation signature of human hippocampus in Alzheimer's disease is linked to neurogenesis.

bioRxiv preprint doi: https://doi.org/10.1101/857953; this version posted November 29, 2019. The copyright holder for this preprint (which was not certified by peer review) is the author/funder. All rights reserved. No reuse allowed without permission.

Clin. Epigenetics 2019;11(1):1–16.

10. Lunnon K, Smith R, Hannon E, et al. Methylomic profiling implicates cortical deregulation of ANK1 in Alzheimer's disease. Nat. Neurosci. 2014;17(9):1164–70.

11. De Jager PL, Srivastava G, Lunnon K, et al. Alzheimer's disease: early alterations in brain DNA methylation at ANK1, BIN1, RHBDF2 and other loci. Nat. Neurosci. 2014;17(9):1156–63.

12. Humphries CE, Kohli MA, Nathanson L, et al. Integrated whole transcriptome and DNA methylation analysis identifies gene networks specific to late-onset Alzheimer's disease. J. Alzheimer's Dis. 2015;44(3):977–987.

13. Watson CT, Roussos P, Garg P, et al. Genome-wide12 DNA methylation profiling in the superior temporal gyrus reveals epigenetic signatures associated with Alzheimer's disease. Genome Med. 2016;8(1):1–14.

14. Bakulski KM, Dolinoy DC, Sartor MA, et al. Genome-wide DNA methylation differences between late-onset alzheimer's disease and cognitively normal controls in human frontal cortex. J. Alzheimer's Dis. 2012;29(3):571–588.

15. Marioni RE, McRae AF, Bressler J, et al. Meta-analysis of epigenome-wide association studies of cognitive abilities. Mol. Psychiatry 2018;23(11):2133–2144.

16. Broadaway KA, Cutler DJ, Duncan R, et al. A Statistical Approach for Testing Cross-Phenotype Effects of Rare Variants. Am. J. Hum. Genet. 2016;98(3):525–540.

17. Holleman AM, Broadaway KA, Duncan R, et al. Powerful and Efficient Strategies for Genetic Association Testing of Symptom and Questionnaire Data in Psychiatric Genetic Studies. Sci. Rep. 2019;9(1):1–11.

18. Bennett DA, Buchman AS, Boyle PA, et al. Religious Orders Study and Rush Memory and Aging Project. [Internet]. J. Alzheimer's Dis. 2018;64(s1):S161–S189.Available from: http://www.ncbi.nlm.nih.gov/pubmed/29865057

bioRxiv preprint doi: https://doi.org/10.1101/857953; this version posted November 29, 2019. The copyright holder for this preprint (which was not certified by peer review) is the author/funder. All rights reserved. No reuse allowed without permission.

490 19. Bennett DA, Wilson RS, Boyle PA, et al. Relation of neuropathology to cognition in
491 persons without cognitive impairment. Ann. Neurol. 2012;72(4):599–609.
492 20. Chen Y, Lemire M, Choufani S, et al. Discovery of cross-reactive probes and
493 polymorphic CpGs in the Illumina Infinium HumanMethylation450 microarray.
494 Epigenetics 2013;8(2):203–9.
495 21. Barfield RT, Almli LM, Kilaru V, et al. Accounting for population stratification in
496 DNA methylation studies. Genet. Epidemiol. 2014;38(3):231–241.
497 22. Teschendorff AE, Marabita F, Lechner M, et al. A beta-mixture quantile normalization
498 method for correcting probe design bias in Illumina Infinium 450 k DNA methylation
499 data. Bioinformatics 2013;29(2):189–196.
500 23. Leek JT, Johnson WE, Parker HS, et al. The sva package for removing batch effects
501 and other unwanted variation in high-throughput experiments. Bioinformatics
502 2012;28(6):882–3.
503 24. Guintivano J, Aryee MJ, Kaminsky ZA. A cell epigenotype specific model for the
504 correction of brain cellular heterogeneity bias and its application to age, brain region
505 and major depression. Epigenetics 2013;8(3):290–302.
506 25. De Jager PL, Shulman JM, Chibnik LB, et al. A genome-wide scan for common
507 variants affecting the rate of age-related cognitive decline. Neurobiol. Aging
508 2012;33(5):1017.e1–15.
509 26. Das S, Forer L, Schönherr S, et al. Next-generation genotype imputation service and
510 methods. Nat. Genet. 2016;48(10):1284–1287.
511 27. Dobin A, Davis CA, Schlesinger F, et al. STAR: ultrafast universal RNA-seq aligner.
512 Bioinformatics 2013;29(1):15–21.
513 28. Love MI, Huber W, Anders S. Moderated estimation of fold change and dispersion for
514 RNA-seq data with DESeq2. Genome Biol. 2014;15(12):550.

bioRxiv preprint doi: https://doi.org/10.1101/857953; this version posted November 29, 2019. The copyright holder for this preprint (which was not certified by peer review) is the author/funder. All rights reserved. No reuse allowed without permission.

29. Newman AM, Liu CL, Green MR, et al. Robust enumeration of cell subsets from tissue expression profiles. Nat. Methods 2015;12(5):453–7.

30. Darmanis S, Sloan SA, Zhang Y, et al. A survey of human brain transcriptome diversity at the single cell level. Proc. Natl. Acad. Sci. U. S. A. 2015;112(23):7285–90.

31. Bennett DA, Schneider JA, Arvanitakis Z, Wilson RS. Overview and findings from the religious orders study. Curr. Alzheimer Res. 2012;9(6):628–45.

32. Bennett DA, Schneider JA, Buchman AS, et al. Overview and findings from the rush memory and aging project. Curr. Alzheimer Res. 2012;9(6):646–663.

33. Braak H, Braak E. Neuropathological stageing of Alzheimer-related changes. Acta Neuropathol 1991;82:239–259.

34. Malani N. hiAnnotator: Functions for annotating GRanges objects. Version 1.12.0. 2017;

35. Paajanen T, Hänninen T, Tunnard C, et al. CERAD neuropsychological compound scores are accurate in detecting prodromal alzheimer's disease: A prospective AddNeuroMed study. J. Alzheimer's Dis. 2014;39(3):679–690.

36. Larson NB, Chen J, Schaid DJ. A review of kernel methods for genetic association studies. Genet. Epidemiol. 2019;43(2):122–136.

37. Wu MC, Lee S, Cai T, et al. Rare-variant association testing for sequencing data with the sequence kernel association test. Am. J. Hum. Genet. 2011;89(1):82–93.

38. Davies RB. Algorithm AS 155: The Distribution of a Linear Combination of $\chi 2$ Random Variables. J. R. Stat. Soc. Ser. C Appl. Stat. 1980;29(3):323–333.

39. Tingley D, Yamamoto T, Hirose K, et al. mediation: R Package for Causal Mediation Analysis. J. Stat. Softw. 2014;59(5):1–38.

40. Imai K, Keele L, Tingley D. A general approach to causal mediation analysis. Psychol. Methods 2010;15(4):309–34.

bioRxiv preprint doi: https://doi.org/10.1101/857953; this version posted November 29, 2019. The copyright holder for this preprint (which was not certified by peer review) is the author/funder. All rights reserved. No reuse allowed without permission.

41. Ikram MA, VanderWeele TJ. A proposed clinical and biological interpretation of mediated interaction. Eur. J. Epidemiol. 2015;30(10):1115–1118.

42. Valeri L, Vanderweele TJ. Mediation analysis allowing for exposure-mediator interactions and causal interpretation: theoretical assumptions and implementation with SAS and SPSS macros. Psychol. Methods 2013;18(2):137–50.

43. Martin TC, Yet I, Tsai PC, Bell JT. coMET: Visualisation of regional epigenome-wide association scan results and DNA co-methylation patterns. BMC Bioinformatics 2015;16(1):1–5.

44. Marques F, Sousa JC, Sousa N, Palha JA. Blood-brain-barriers in aging and in Alzheimer's disease. Mol. Neurodegener. 2013;8:38.

45. Farrall AJ, Wardlaw JM. Blood-brain barrier: ageing and microvascular disease--systematic review and meta-analysis. Neurobiol. Aging 2009;30(3):337–52.

46. Viggars AP, Wharton SB, Simpson JE, et al. Alterations in the blood brain barrier in ageing cerebral cortex in relationship to Alzheimer-type pathology: a study in the MRC-CFAS population neuropathology cohort. Neurosci. Lett. 2011;505(1):25–30.

47. Weiss N, Miller F, Cazaubon S, Couraud P-O. The blood-brain barrier in brain homeostasis and neurological diseases. Biochim. Biophys. Acta 2009;1788(4):842–57.

48. Boyle PA, Yu L, Leurgans SE, et al. Attributable risk of Alzheimer's dementia attributed to age-related neuropathologies. Ann. Neurol. 2019;85(1):114–124.

bioRxiv preprint doi: https://doi.org/10.1101/857953; this version posted November 29, 2019. The copyright holder for this preprint (which was not certified by peer review) is the author/funder. All rights reserved. No reuse allowed without permission.

Tables

Table 1. Study characteristics of the discovery (ROS/MAP) and replication datasets.

	Discovery Dataset	**Replication Dataset**
N	636	66
Age at death, mean ± sd	86.22 ± 4.72	87.48 ± 6.57
Female, n (%)	401 (63.1%)	44 (66.67%)
Ancestry		
European, n (%)	621 (97.6%)	*n.a.*
African American, n (%)	11 (1.7%)	*n.a.*
Native American, n (%)	1 (0.2%)	*n.a.*
Asian, n (%)	3 (0.5%)	*n.a.*
Years of education, mean ± sd	16.63 ± 3.54	*n.a.*
Never smoker, n (%)	444 (69.8%)	*n.a.*
Ex-smoker, n (%)	176 (27.7%)	*n.a.*
Smoker, n (%)	16 (2.5%)	*n.a.*
Post mortem interval (PMI), mean ± sd	7.43 ± 5.79	*n.a.*
Decline in episodic memory, mean ± sd	-0.03 ± 0.11	*n.a.*
Decline in perceptual speed, mean ± sd	-0.02 ± 0.08	*n.a.*
Decline in perceptual orientation, mean ± sd	-0.01 ± 0.04	*n.a.*
Decline in semantic memory, mean ± sd	-0.03 ± 0.13	*n.a.*
Decline in working memory, mean ± sd	-0.01 ± 0.05	*n.a.*
CERAD, mean ± sd	2.27 ± 1.15	*n.a.*
Braak stage, mean ± sd	3.44 ± 1.26	4.70 ± 1.62

n.a.: information not available in replication dataset.

Table 2. Top signals (p-values < 5 x 10^{-5}) for the association between DNA methylation and cognitive decline across all domains as well as in the single domains in the discovery dataset (ROS/MAP).

gene	chr	pos (lower)	pos (upper)	mean dist gene	max dist gene	#CpG sites	p-value (across all domains)	p-value (EM)	p-value (PS)	p-value (PO)	p-value (SM)	p-value (WM)
CLDN5	chr22	19510877	19515608	1030	2062	18	**9.96E-07**	4.65E-06	7.16E-05	0.0021	2.35E-05	**2.54E-07**
AC084018.1	chr12	122235169	122241475	501	1414	15	2.84E-06	5.96E-05	0.0001	0.0060	4.13E-06	0.0002
CTB-186G2.1	chr19	39087135	39090701	692	1633	4	6.19E-06	7.33E-06	3.50E-05	0.0015	7.45E-05	7.69E-05
ATG16L2	chr11	72521478	72546168	1326	12094	25	8.22E-06	1.32E-05	0.0002	0.0086	8.31E-05	0.0004
KCNN4	chr19	44270892	44286076	1682	6854	13	1.01E-05	2.01E-05	0.0002	0.0127	0.0001	4.12E-05
RP11-779O18.1	chr5	172168177	172189374	7685	17051	12	1.86E-05	1.26E-05	0.0002	0.0262	0.0009	3.18E-06
TTC22	chr1	55240609	55268659	1189	4775	23	3.42E-05	0.000192	0.0002	0.0182	0.0002	6.16E-05
DCUN1D2-AS	chr13	114123258	114129580	2530	3583	10	3.87E-05	5.91E-06	0.0004	0.0176	0.0014	4.48E-05
PNMA1	chr14	74177136	74181427	777	1357	9	3.88E-05	3.14E-05	0.0079	0.0030	0.0002	0.0006
RP11-101C11.1	chr1	55682652	55709508	5270	9658	2	3.99E-05	2.36E-05	0.0004	0.0565	0.0006	0.0003

EM: decline in episodic memory; PS: decline in perceptual speed; PO: decline in perceptual orientation; SM: decline in semantic memory; WM: decline in working memory
Adjusted for age at death, education, sex, ancestry, smoking status, post-mortem interval (PMI) and the first three principal components (PCs).
Bonferroni threshold: 0.05/26,558=1.88x10^{-6} (p-values below Bonferroni threshold in **bold**)
Suggestive: p-values < 5x10^{-5} (underlined)

bioRxiv preprint doi: https://doi.org/10.1101/857953; this version posted November 29, 2019. The copyright holder for this preprint (which was not certified by peer review) is the author/funder. All rights reserved. No reuse allowed without permission.

Table 3. Validation of ROS/MAP (discovery dataset) findings in replication dataset

				Discovery Dataset				Replication Dataset		
gene	**chr**	**pos (lower)**	**pos (upper)**	**#CpG sites**	**p-value cognitive decline**	**p-value CERAD**	**p-value Braak**	**#CpG sites**	**p-value Braak**	**p-value Braak (permutation Test[1])**
CLDN5	chr22	19510877	19515608	18	9.96E-07	**0.0023**	**0.0066**	18	**0.0088**	**0.0076**
AC084018.1	chr12	122235169	122241475	15	2.84E-06	**0.0002**	**5.31E-06**	16	0.1794	0.1791
CTB-186G2.1	chr19	39087135	39090701	4	6.19E-06	**0.0005**	**8.36E-05**	4	**0.0125**	**0.0121**
ATG16L2	chr11	72521478	72546168	25	8.22E-06	**0.0003**	**5.67E-06**	25	0.1535	0.1536
KCNN4	chr19	44270892	44286076	13	1.01E-05	**0.0028**	**0.0001**	15	**0.0222**	**0.0178**
RP11-779O18.1	chr5	172168177	172189374	12	1.86E-05	**0.0168**	**0.0008**	12	0.0890	0.0872
TTC22	chr1	55240609	55268659	23	3.42E-05	**0.0010**	**0.0002**	24	0.2027	0.2096
DCUN1D2-AS	chr13	114123258	114129580	10	3.87E-05	**0.0363**	**0.0344**	11	0.6988	0.7057
PNMA1	chr14	74177136	74181427	9	3.88E-05	0.0709	0.1913	10	0.1022	0.0999
RP11-101C11.1	chr1	55682652	55709508	2	3.99E-05	0.1052	0.0831	2	0.1582	0.1654

Discovery dataset: ROS/MAP samples. All analyses were adjusted for age at death, education, sex, ancestry, smoking status, post-mortem interval (PMI) and the first three principal components (PCs). Associations with CERAD were additionally adjusted for cell type proportions and the fourth PC.
Replication dataset: MRC Brain Bank Samples (Lunnon et al., 2014) All analyses were adjusted for age at death, sex and cell type composition.
Successful replication (p-value < 0.05 in validation cohort) in **bold**.
[1]Due to the small sample size (N=66) we conducted a permutation test with 10,000 replications in addition to the Davies' approximation to verify the p-values in the validation cohort.

bioRxiv preprint doi: https://doi.org/10.1101/857953; this version posted November 29, 2019. The copyright holder for this preprint (which was not certified by peer review) is the author/funder. All rights reserved. No reuse allowed without permission.

Table 4. Identification of lead signals within *CLDN5* and direction of associations.

gene	chr	pos	CpG site	beta (EM)	p-value (EM)	beta (PS)	p-value (PS)	beta (PO)	p-value (PO)	beta (SM)	p-value (SM)	beta (WM)	p-value (WM)
CLDN5	chr22	19512903	cg05460329	-0.93	1.43E-06	-0.62	1.60E-05	-0.25	0.0003	-1.10	1.89E-06	-0.45	2.41E-06
CLDN5	chr22	19512942	cg05498726	-0.55	0.0001	-0.36	0.0008	-0.13	0.0162	-0.61	0.0005	-0.26	0.0002
CLDN5	chr22	19513006	cg11450827	-0.60	0.0007	-0.35	0.0064	-0.16	0.0111	-0.65	0.0019	-0.30	0.0005
CLDN5	chr22	19513008	cg17583256	-0.57	0.0005	-0.30	0.0129	-0.14	0.0180	-0.51	0.0086	-0.27	0.0008
CLDN5	chr22	19513017	cg16773741	-0.76	**1.48E-08**	-0.39	8.38E-05	-0.18	0.0003	-0.86	**8.81E-08**	-0.38	**8.66E-09**
CLDN5	chr22	19513078	cg14553765	-0.44	0.0014	-0.32	0.0017	-0.13	0.0087	-0.60	0.0003	-0.29	1.92E-05
CLDN5	chr22	19513176	cg00189989	-0.61	0.0004	-0.42	0.0009	-0.14	0.0224	-0.78	0.0001	-0.36	1.86E-05

Only CpG sites with a p-value < 0.001 for at least one cognitive domain are shown. Bonferroni threshold: 0.05/338,036=1.48e-07 (p-values below Bonferroni threshold in bold). EM: decline in episodic memory; PS: decline in perceptual speed; PO: decline in perceptual orientation; SM: decline in semantic memory; WM: decline in working memory. Adjusted for age at death, education, sex, ancestry, smoking status, post-mortem interval (PMI) and the first four principal components.

bioRxiv preprint doi: https://doi.org/10.1101/857953; this version posted November 29, 2019. The copyright holder for this preprint (which was not certified by peer review) is the author/funder. All rights reserved. No reuse allowed without permission.

bioRxiv preprint doi: https://doi.org/10.1101/857953; this version posted November 29, 2019. The copyright holder for this preprint (which was not certified by peer review) is the author/funder. All rights reserved. No reuse allowed without permission.

Figure Legends

Figure 1. DNA methylation and cognitive decline. Association between DNA methylation and cognitive decline in ROS/MAP (discovery dataset) tested with GAMuT. Adjusted for age at death, education, sex, ancestry, smoking status, post-mortem interval (PMI) and the first three principal components.

Figure 2. Fine mapping of the association between DNA methylation and decline in working memory. Results from linear regression analyses on the association between CpG sites and cognitive decline in ROS/MAP (discovery dataset) adjusted for age at death, education, sex, ancestry, smoking status, post-mortem interval (PMI) and the first four principal components. The most significant CpG site (cg16773741) is marked in purple and CpG sites associated with genotypes in the same window are marked in yellow (compare Table S17).

Figure 3. Interaction analysis. Associations between DNA methylation of the top CpG site of *CLDN5* (cg16773741) and cognitive trajectory are shown in participants with no to little (category 0) vs. moderate to severe (category 1) signs of neuropathology. No to little signs of neuropathology are defined as a CERAD measure of 3 (possible) or 4 (no AD) or a Braak stage of 0 to II. Moderate to severe signs of neuropathology are defined as a CERAD measure of 1 (definite) or 2 (probable) or a Braak stage of III to VI. P-values are given for the test of deviations of the association between methylation in cognitive trajectory between the two strata. The bars present the distribution of the neuropathological variables. EM: decline in episodic memory; PS: decline in perceptual speed; PO: decline in perceptual orientation; SM: decline in semantic memory; WM: decline in working memory. Adjusted for age at death, education, sex, ancestry, smoking status, post-mortem interval (PMI) and the first three principal components.

Figure 4. Causal mediation analysis. Beta-estimates and 95%-confidence intervals of the estimated average causal mediation effects, the average direct effects as well as the total effects. Proportion (with 95%-confidence interval) of the association between DNA methylation (DNAm) of the top CpG site of *CLDN5* (cg16773741) and cognitive trajectory, which is mediated through neuropathology (CERAD & Braak stage) is given in percent. EM: decline in episodic memory; PS: decline in perceptual speed; PO: decline in perceptual orientation; SM: decline in semantic memory; WM: decline in working memory. Adjusted for age at death, education, sex, ancestry, smoking status, post-mortem interval (PMI) and the first three principal components (PCs).

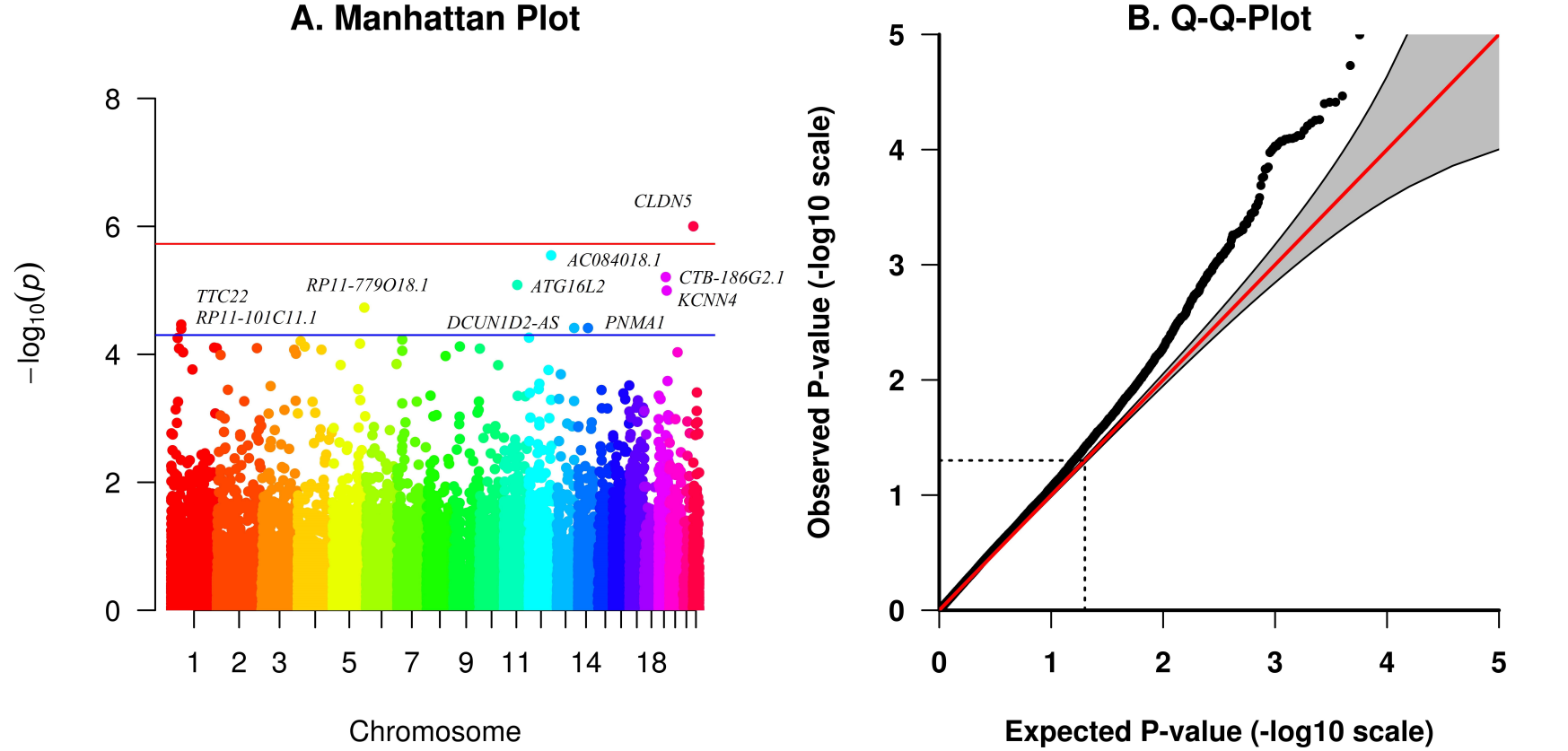
A. Manhattan Plot
−log10(p)
8
6
4
2
0
CLDN5
AC084018.1
CTB-186G2.1
KCNN4
ATG16L2
RP11-779O18.1
TTC22
RP11-101C11.1
DCUN1D2-AS
PNMA1
1
2
3
5
7
9
11
14
18
Chromosome
B. Q-Q-Plot
Observed P-value (-log10 scale)
5
4
3
2
1
0
0
1
2
3
4
5
Expected P-value (-log10 scale)

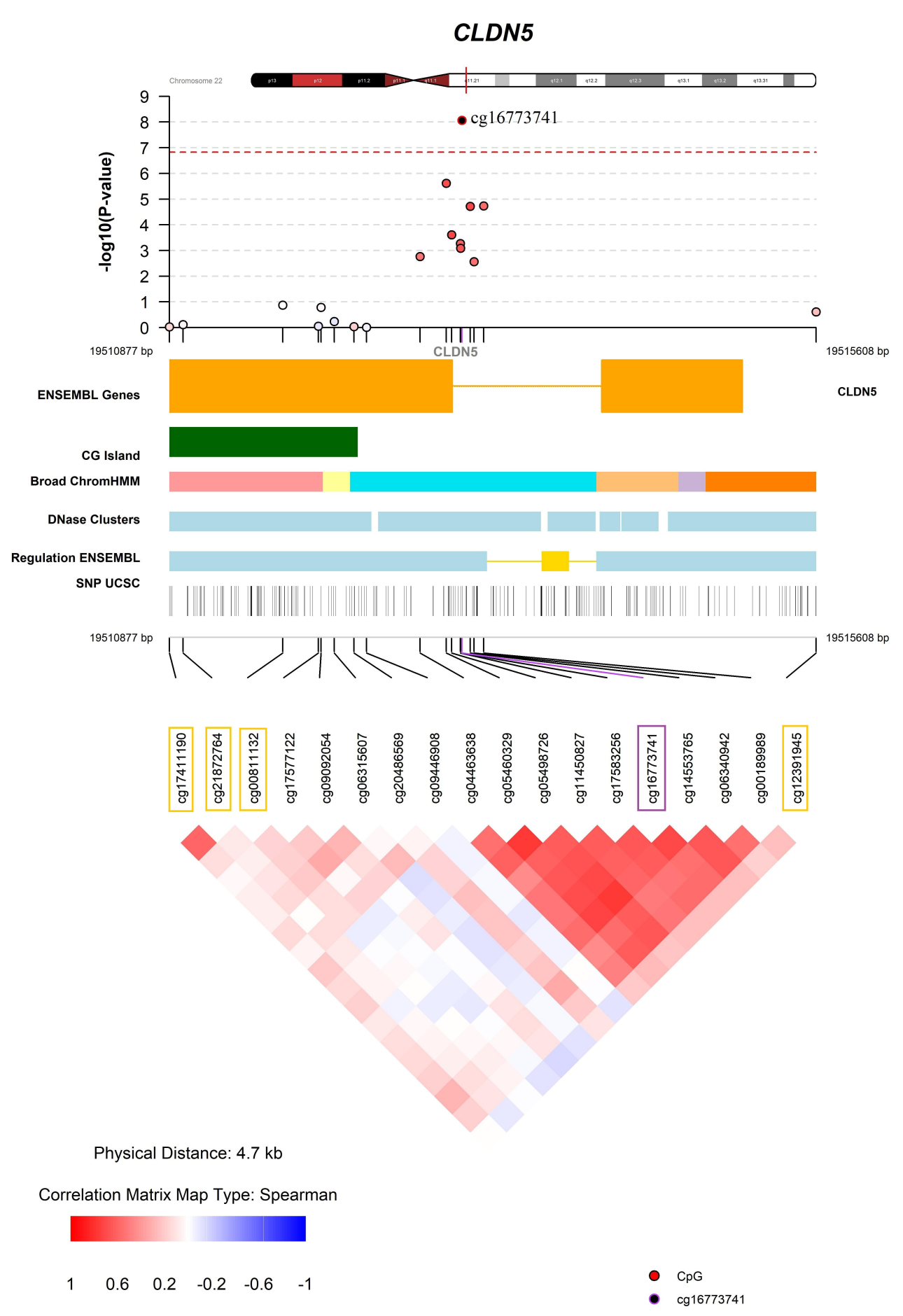
CLDN5
Chromosome 22
cg16773741
-log10(P-value)
19510877 bp
CLDN5
19515608 bp
ENSEMBL Genes
CLDN5
CG Island
Broad ChromHMM
DNase Clusters
Regulation ENSEMBL
SNP UCSC
cg17411190
cg21872764
cg00811132
cg17577122
cg09092054
cg06315607
cg20486569
cg09446908
cg04463638
cg05460329
cg05498726
cg11450827
cg17583256
cg16773741
cg14553765
cg06340942
cg00189989
cg12391945
Physical Distance: 4.7 kb
Correlation Matrix Map Type: Spearman
1 0.6 0.2 -0.2 -0.6 -1
CpG
cg16773741

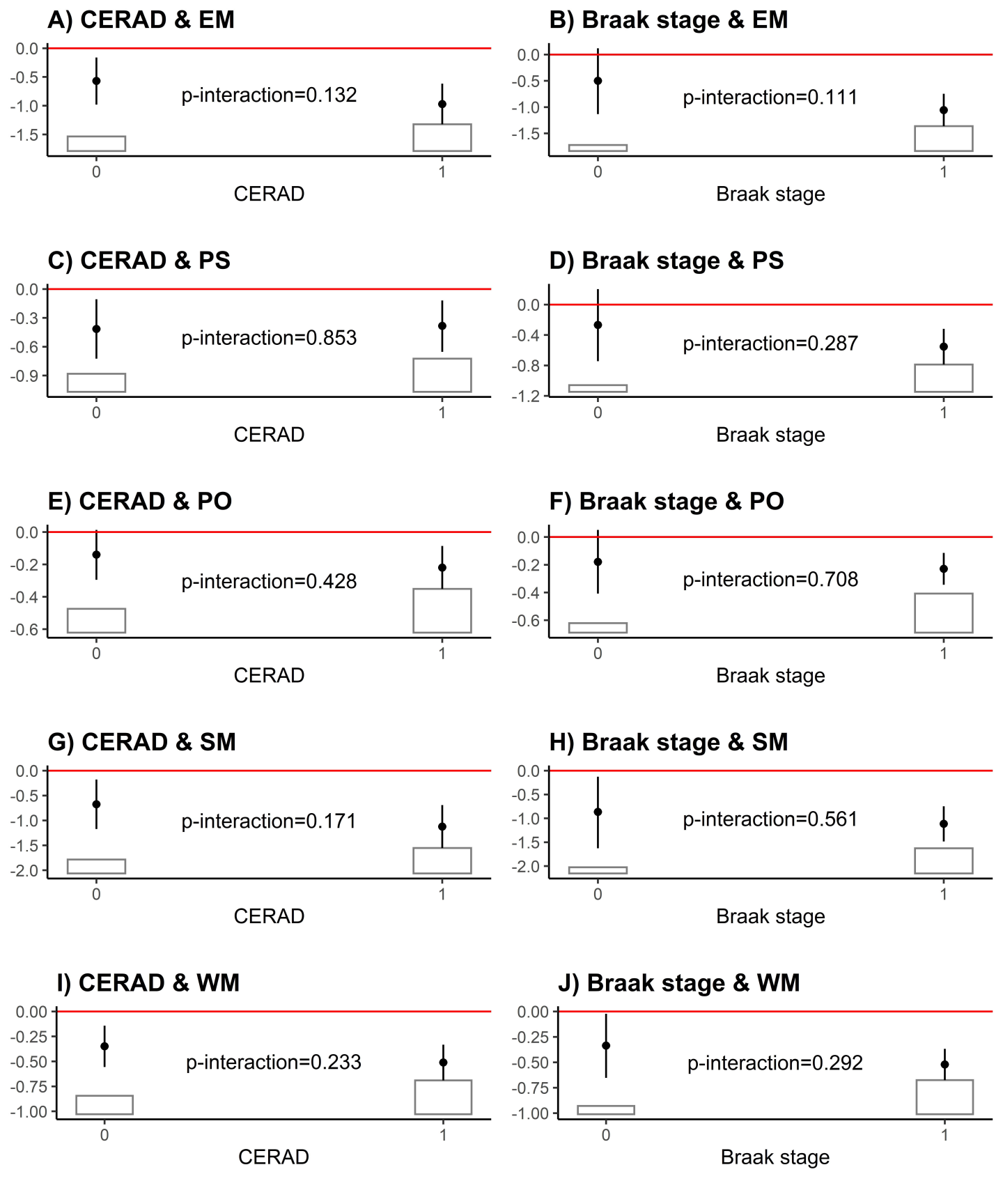
A) CERAD & EM
p-interaction=0.132
CERAD
B) Braak stage & EM
p-interaction=0.111
Braak stage
C) CERAD & PS
p-interaction=0.853
CERAD
D) Braak stage & PS
p-interaction=0.287
Braak stage
E) CERAD & PO
p-interaction=0.428
CERAD
F) Braak stage & PO
p-interaction=0.708
Braak stage
G) CERAD & SM
p-interaction=0.171
CERAD
H) Braak stage & SM
p-interaction=0.561
Braak stage
I) CERAD & WM
p-interaction=0.233
CERAD
J) Braak stage & WM
p-interaction=0.292
Braak stage

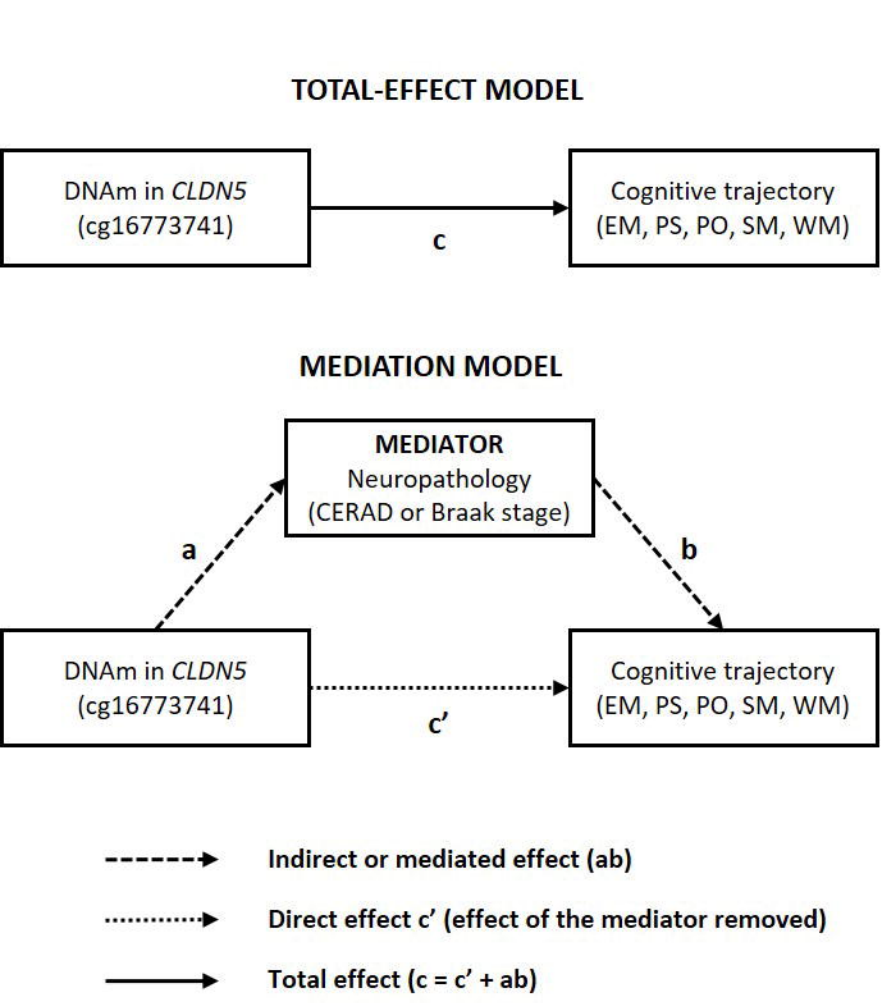
TOTAL-EFFECT MODEL
DNAm in CLDN5 (cg16773741)
c
Cognitive trajectory (EM, PS, PO, SM, WM)
MEDIATION MODEL
MEDIATOR
Neuropathology
(CERAD or Braak stage)
a
b
DNAm in CLDN5 (cg16773741)
c'
Cognitive trajectory (EM, PS, PO, SM, WM)
Indirect or mediated effect (ab)
Direct effect c' (effect of the mediator removed)
Total effect (c = c' + ab)

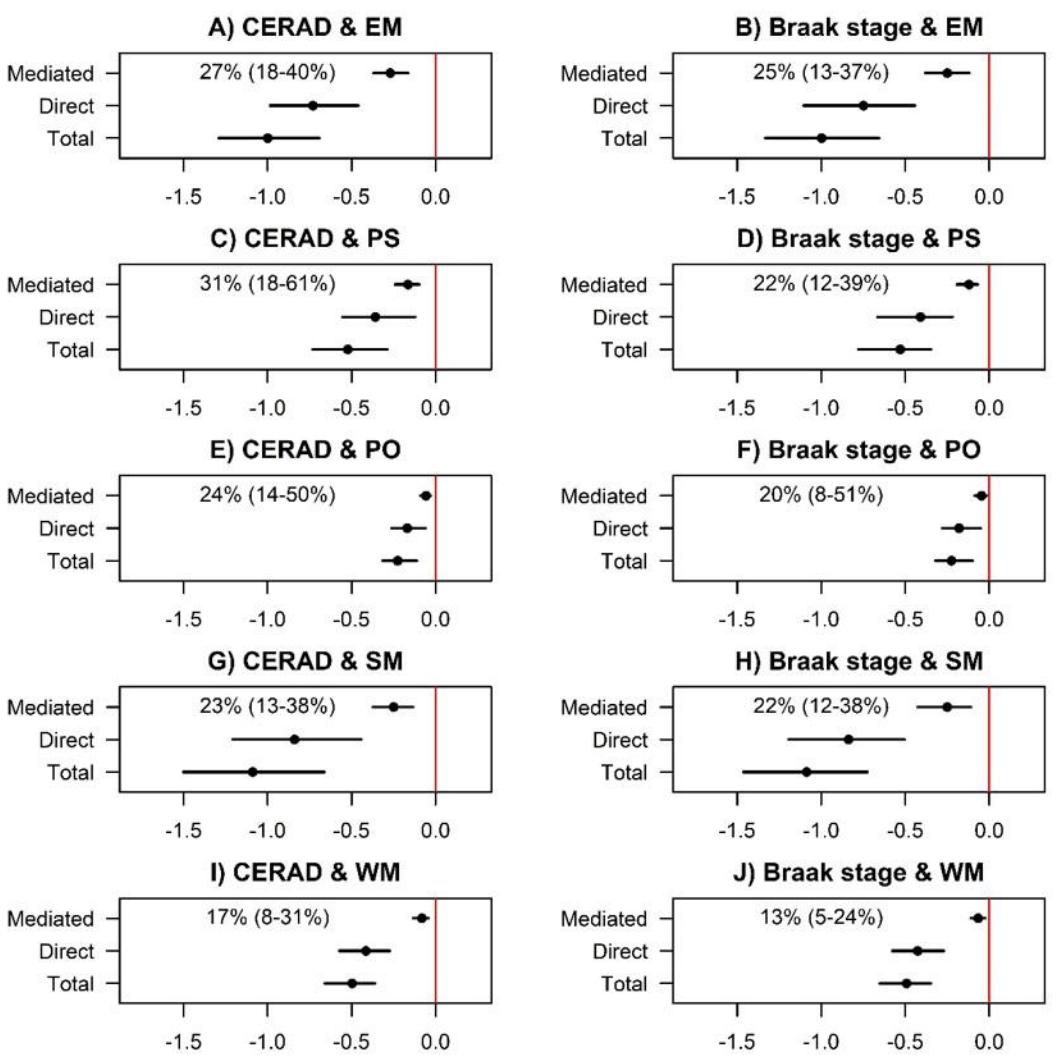
A) CERAD & EM
27% (18-40%)
B) Braak stage & EM
25% (13-37%)
C) CERAD & PS
31% (18-61%)
D) Braak stage & PS
22% (12-39%)
E) CERAD & PO
24% (14-50%)
F) Braak stage & PO
20% (8-51%)
G) CERAD & SM
23% (13-38%)
H) Braak stage & SM
22% (12-38%)
I) CERAD & WM
17% (8-31%)
J) Braak stage & WM
13% (5-24%)
Mediated
Direct
Total
-1.5
-1.0
-0.5
0.0